# Fluorescence Tracking of Genome Release during the Mechanical Unpacking of Single Viruses

Ortega-Esteban, Alvaro ; Bodensiek, Kai ; San Martín, Carmen ; Suomalainen, Maarit ; Greber, Urs F ; de Pablo, Pedro J ; Schaap, Iwan A T

Abstract: Viruses package their genome in a robust protein coat to protect it during transmission between cells and organisms. In a reaction termed uncoating, the virus is progressively weakened during entry into cells. At the end of the uncoating process the genome separates, becomes transcriptionally active, and initiates the production of progeny. Here, we triggered the disruption of single human adenovirus capsids with atomic force microscopy, and followed genome exposure by single molecule fluorescence microscopy. This method allowed the comparison of immature (non-infectious) and mature (infectious) adenovirus particles. We observed two condensation states of the fluorescently labeled genome, a feature of the virus that may be related to infectivity. Beyond tracking the unpacking of virus genomes this approach may find application in testing the cargo release of bio-inspired delivery vehicles.

DOI: https://doi.org/10.1021/acsnano.5b03020

# Fluorescence tracking of genome release during mechanical unpacking of single viruses

Alvaro Ortega-Esteban[1, §], Kai Bodensiek[2, §], Carmen San Martín[3], Maarit Suomalainen[4], Urs F. Greber[4], Pedro J. de Pablo[1, 5], Iwan A.T. Schaap[2, 6]

[1] Departamento de Física de la Materia Condensada, Universidad Autónoma de Madrid, Spain

[2] III. Physikalisches Institut, Georg August Universität, Göttingen, Germany

[3] Department of Macromolecular Structures and NanoBioMedicine Initiative, Centro Nacional de Biotecnología (CNB-CSIC), Madrid, Spain

[4] Institute of Molecular Life Sciences, University of Zürich, Switzerland

[5] Condensed Matter Physics Center (IFIMAC), Universidad Autónoma de Madrid, Spain

[6] Center for Nanoscale Microscopy and Molecular Physiology of the Brain (CNMPB), Göttingen, Germany

[§] Equal contribution

**Corresponding author**

Pedro J. de Pablo p.j.depablo@uam.es

Iwan A.T. Schaap ischaap@gwdg.de

**Keywords**

AFM, Single molecule fluorescence, TIRF, mechanics, nanoparticle, adenovirus, uncoating, drug delivery

**Abstract**

Viruses package their genome in a robust protein coat to protect it during transmission between cells and organisms. In a reaction termed uncoating, the virus is progressively weakened during entry into cells. At the end of the uncoating process the genome separates, becomes transcriptionally active, and initiates the production of progeny. Here, we triggered the disruption of single human adenovirus capsids with atomic force microscopy, and followed genome exposure by single molecule fluorescence microscopy. This method allowed the comparison of immature (non-infectious) and mature (infectious) adenovirus particles. We observed two condensation states of the fluorescently labeled genome, a feature of the virus that may be related to infectivity. Beyond tracking the unpacking of virus genomes this approach may find application in testing the cargo release of bio-inspired delivery vehicles.

**Introduction**

Viruses present an elegant solution for packing, transporting and delivering nucleic acids into hosts [1]. They inspired the design of transporters of artificial cargo with applications from nanomedicine to synthetic biology.[2, 3] The success of both viruses and artificial transporters relies on their ability to shield the cargo and to release it at the right location. Misdelivery of genomes can provoke innate immunity reactions and prevent viral replication.[4] Viruses that infect eukaryotic cells usually undergo structural changes leading to complete capsid disassembly and release of the viral genome.[5-7] Conformational transitions in the capsid can be triggered by cellular cues, such as receptor binding, the ionic environment, or mechanical cues.[8-11] Whether the released cargo carries out its designated function depends not only on its protection by the capsid but, in many cases, also requires a maturation step to render the cargo active.[12-15] Thus, a better understanding of the mechanisms that both viruses and artificial nanoparticles employ for cargo delivery, demands an integrated approach involving structural dynamics of the capsid, and the physical state of the cargo.

We addressed the uncoating of human adenovirus, a non-enveloped 95 nm large icosahedral virus with a double stranded DNA (dsDNA) genome.[16] During transmission the viral genome is protected and condensed as a core within the capsid coat (figure 1a). Uncoating starts at the plasma membrane of the target cell. Here, the virus binds with its fibers to mobile receptor molecules (CAR), while the penton fiber-bases interact with confined secondary receptor molecules (integrins).[9, 17, 18] The combined mechanical interactions result in fiber shedding, and presumably also penton release. This facilitates the liberation of a fraction of the viral membrane lytic protein VI, which forms small pores in the plasma membrane.[19] These pores are too small for the virus to penetrate, but they trigger a membrane repair process which eventually leads to the uptake of the virus in endosomes. The membrane lytic function of protein VI is enhanced by an increase of cellular ceramide lipid levels which leads to an early rupture of the endosomal membrane, notably in a pH independent manner.[19-22] Upon access to the cytosol, the viral genome remains in a partially disrupted capsid which is transported along microtubules by motor-proteins to the nuclear pore complexes where it docks.[23-27] At the nuclear pore complex, the genome is released by mechanical forces arising from the antagonistic action of kinesin motor-proteins against the holding force of the nuclear pore complex where the virus is attached.[10]

Both phases of disassembly have been demonstrated by cryo-electron tomography in purified adenovirus particles.[28] Upon thermal or acidic stress, mildly disrupted particles lacking a few pentons and peripheral core material were observed. Under harsher conditions the capsid shell cracked open and the viral genome was released in a highly cooperative way. Intriguingly, single molecule fluorescence experiments on infected cells showed that single adenovirus genomes separated from the capsid appeared slightly larger in size than the capsid enclosed genome.[27] This suggests some sort of decondensation of the genome upon release from the capsid.

Since the early 2000s, Atomic Force Microscopy (AFM) has emerged as a unique technique to measure mechanical stability of protein cages in a near physiological liquid environment.[29] By indenting single protein shells with the AFM probe the elasticity and failure limits of many different protein cages have been measured.[30-32] This showed that many virus protein capsids behave like elastic and robust nanocontainers.[33, 34] AFM has also been used to track the

disassembly process of virus capsids by measuring the structural transitions triggered by changes in pH.[7, 35] Furthermore, AFM has been used to apply well-controlled forces to single capsids to trigger capsid disruption. For adenovirus, AFM-induced disruption follows the same sequence as the uncoating *in vivo*, starting with release of pentons, followed by capsid disruption at increasing mechanical force.[36]

Here we aimed to better understand how the DNA genome is released from adenovirus during mechanical disassembly. The adenovirus genome is a mini-chromosome composed of a 35 kbp long dsDNA molecule and about 25 MDa of condensing proteins.[37-41] The exact architecture of this DNA-protein core is unknown. Adenoviruses assemble in the nucleus of the infected cell, and require a maturation step to become infectious.[42, 43] During this step, the viral protease (AVP) which is packed in the capsid, cleaves the condensing proteins along with other capsid proteins[42, 44], which leads to a change in the organization of the viral core as observed by electron microscopy.[28, 45] The temperature sensitive adenovirus mutant TS1 fails to package functional protease, contains uncleaved core proteins, and is not infectious.[43] In earlier work, based on AFM imaging, we found that after mechanical rupturing of virus capsids, the viral core of the TS1 mutant remained visible as a condensed blob whereas the core of the WT virus could not be resolved.[36] These results already suggested a difference in core organization which could lead to different diffusive behavior of the genome after uncoating. To follow up this speculation we combined AFM and single molecule fluorescence microscopy to specifically observe genome uncoating from wild type and TS1 adenovirus. The combination of these techniques allows simultaneous manipulation and imaging of samples, which can be applied for the measurement of mechanical properties of single proteins and the identification of specific components in complex assemblies.[46-48] Upon disassembling single viruses, we find that the core of the wild type virus (mature) expands more and has better accessibility to the fluorescent dye than the TS1 core (immature), which indicates a loosening of its architecture upon maturation. This loss of structural organization may be important for viral transcription in the cell nucleus.

## Results

*Combining single molecule fluorescence with high resolution AFM*

We used the AFM probe to crack open single viral capsids. The genome exposure was tracked with a DNA specific intercalating fluorescent dye (YOYO-1) that could only access the DNA after the capsid had been opened up (figure 1b). To be able to collect fluorescent signals from the released virus genomes during AFM manipulation we integrated a single molecule fluorescence microscope in our AFM. To minimize increase of AFM noise, induced by the added components for fluorescence microscopy, we optimized the opto-mechanical design. Both the camera and the excitation laser were mechanically and thermally isolated from the AFM to limit heat and vibration transmission (Figure 2a). Figure 2b shows that in this configuration both mature and immature human adenoviruses can be imaged with AFM in buffer at sufficient high resolution to clearly resolve the icosahedral structure. To excite only the fluorescent dye molecules close to the surface we used a total internal reflection fluorescence (TIRF) layout. This is necessary to minimize the background signal from the AFM probe itself that remains largely out of the evanescent excitation field.[49] For the mechanical unpacking measurements with AFM, the viral capsids need to be firmly immobilized via $Ni^{2+}$ ions to freshly cleaved mica substrates.[36] To enable the use of a high numerical aperture (NA) microscope objective for fluorescent imaging, we glued a thin disc of mica onto a microscope coverslip (see methods). Figure S1 shows that this solution provides single fluorescent molecule sensitivity in the presence of the AFM probe.

*Slow genome unpacking*

First, we verified that we could monitor the exposure of the viral genome during gradual mechanical uncoating of the virus. To this end we mimicked the uncoating process of human adenoviruses with fatigue experiments. Single capsids were repeatedly subjected to small indentations below the rupture strength, which ultimately resulted in a stepwise disruption of the shell.[36] Figure 3 and movie S1 show a mechanical fatigue experiment performed on a mature adenovirus particle. YOYO-1, which shows an increase in fluorescence intensity of 3 orders of magnitude upon binding dsDNA[50], was present in the buffer at 300 nM to monitor the exposure of the genome. The virus was imaged 21 times (where each scan line was performed forward and

backward). After each scan, the fluorescence intensity was collected to monitor genome exposure. The first AFM frame in figure 3a shows the scan of the intact viral particle. The first fluorescence frame presents background noise confirming that the capsid is intact and the dsDNA is inaccessible to YOYO-1. In AFM frame 7, the viral particle has lost its first vertex capsomer (penton, indicated with a circle). In the corresponding fluorescence frame 7 a dim intensity spot appeared, which remained stable until frame 16. From AFM frame 17 new defects appeared until at frame 21 the particle was completely disrupted. The corresponding fluorescence frames show that the emission intensity (figure 3b) increases with capsid disruption, which indicates that the DNA genome becomes increasingly accessible to YOYO-1 and remains co-localized with the capsid. The genome itself remains invisible in the AFM scans due to its softness and mobility. This experiment shows that the method is sensitive enough to detect the release of a single pentameric capsomer via an increase in fluorescence intensity.

*Fast genome unpacking*

Because capsid disassembly during fatigue experiments is a stochastic process[36] the slow genome unpacking assay would result in a distribution of capsids at various stages of uncoating and thus in a high variability of the fluorescent signals obtained from different particles. To synchronize disassembly, we sought a method for fast removal of the capsid, so that we could investigate the physical state of the viral genome itself. The AFM scans in figure 4 a show that the capsid can be completely disrupted within 0.5 s by performing a single force curve with a maximum force of around 15 nN, well above the rupture strength of the capsid[28] (see methods). Prior to the force curve the capsid was intact, while afterward it was completely disassembled leaving the viral core exposed. Figure 4a shows that no fluorescent signal was present before the force curve while afterward a bright spot appeared due to the viral genome becoming accessible to the YOYO-1 dye. The corresponding time trace of the experiment (figure 4b) confirms that the intensity of the fluorescence signal increases at the moment when the high force is applied, and remains high after the AFM probe has retracted (Movie S2). With the fast unpacking assay we can synchronize the fluorescence intensity curves with sub-second accuracy which provides a method to investigate the changes in genome organization in more detail.

*Maturation increases the accessibility of the adenovirus core for YOYO-1 molecules*

To investigate if the structural differences between the viral cores of the mature and immature viruses have an effect on their diffusion after release, we repeated the fast genome unpacking assay on both viruses. If the viral core remains compact after unpacking, which we expect for the immature particle, it will be difficult for the dye to access binding sites. If, on the other hand, the nucleoprotein complex expands after unpacking, binding of the dye to the DNA will be enhanced. We performed fast unpacking experiments on 16 mature and 17 immature adenovirus particles and recorded the fluorescence intensity for 80 seconds after opening the capsids. Figure 4c shows the average fluorescence emission for both cases. Consistent with the behavior shown in figure 4b, the emission rises sharply after rupturing the capsids and continues to increase slowly afterward. This increase represents the average rate of binding minus bleaching of the YOYO-1 molecules. Under our conditions, the binding rate of new YOYO-1 molecules is higher than their bleaching rate. The averaged signal for the mature genomes is higher than that of the immature genomes. This agrees with a looser organization of the mature genome which leads to a better accessibility for the dye.

*The mature adenovirus core expands after release*

To further evaluate the possible expansion of the mature genome after fast unpacking, we measured the size of the fluorescent spot. The diffraction limited resolution of our optical system restricts the size of the smallest spot that we can observe to a radius of about 200 nm which is larger than the intact virus (95 nm). However, if the labeled sample is a collection of spatially spread point sources, this will lead to a dilation of the imaged spot from which we can estimate the expansion of the viral core. We quantified the width by fitting a 2D Gaussian function to the imaged fluorescent spots. When we compared the spot sizes from 100 nm and 200 nm diameter fluorescent beads we found an increase in width from 208 nm to 253 nm (Figure S2). To compare the genome condensation state in both virus types we determined the spot size in each frame of all fluorescence movies. Figure 5a shows the average fits for all movies, revealing that the mature core shows a spot width of 295 nm, which is much larger than the 229 nm of the immature core. This expansion of 66 nm represents a lower limit, while further diffusion of the genome may be hindered by the surface-immobilized remainder of the capsid as shown in Figure

4a. To investigate the temporal evolution of the core expansion we plotted the fitted width of each frame as a function of time. Figure 5b shows that the expansion occurs directly after opening the capsid with the AFM probe and remains fairly constant afterward. The apparent width of the mature genome was more variable at the beginning of the observation, and became smaller after ~20 s, possibly suggesting photocleavage of mobile extended parts of the genome.[51]

## Discussion

Compared to cells, viruses contain 2 to 3 times less water[52], and are tightly packed assemblies of proteins and nucleic acids, sometimes wrapped with lipids and sugars. The nucleic acid is well protected and condensed within the tight space of the viral capsid. Breaking up the capsid after the virus enters the host cell is key to infection. Capsid dismantling is triggered by host factors such as receptors, components of the endocytic machinery, and changes in the ionic or mechanical environment, allowing the release of the genome.[11] Here, we used mechanical cues to open the adenovirus capsid and fluorescence imaging to track the release of the viral DNA. Our results show that the tightly packed core of the adenovirus expands after the final steps of uncoating. Ultimately, genome decondensation is crucial to grant access to components of the DNA/RNA metabolism machinery whose action is required for virus propagation. The temporally controlled decondensation of the viral genome might be a general feature of viruses to limit recognition of their genomes by innate and intrinsic immune factors. In the case of human adenovirus this involves endosomal and cytosolic DNA sensors that lead to inflammation and the production of interferon.[53] Understanding the dynamics of viral genome decondensation should therefore open new avenues to interfere with virus propagation. For example, it has been shown that inorganic transition metal complexes that cause condensation of viral dsDNA improve survival of adenovirus infected cells.[54]

The transient and dynamic nature of uncoating presents a significant challenge for investigations at the molecular level. Ensemble experiments to monitor genome release have been performed with bacteriophages.[55] Genome release of human adenovirus has been measured in bulk by fluorescent detection of the genomes after thermal or chemical disruption of the capsids.[28, 45, 56] At the single particle level, DNA ejection has been visualized in bacteriophages and herpesviruses.[57, 58] Although AFM has been successful in imaging the disassembly of viral capsids[36, 59], the release of the relatively soft and mobile nucleic acid molecules remained largely invisible in such experiments because AFM imaging demands an immobilized sample. Nevertheless, our earlier AFM-only uncoating experiments on adenoviruses suggested that the core of the TS1 mutant retained a compact organization after capsid rupture as compared to the wild type core, which remained largely invisible.[36] Because AFM imaging does not allow

discrimination between molecules that lack distinctive morphological features, an indisputable detection of the viral genome and its dynamics was not possible in these experiments.

Single molecule fluorescence allows specific tracking of DNA dynamics and provides a tool to visualize genome release. Tracking experiments of single viruses in cells have shown that the viral genome is already exposed to the cytosol before the capsid docks at the nuclear pore complex.[27] Viral genome accessibility measurements using click-chemistry demonstrated that early on during virus entry, the DNA is accessible to small organic probes, which implies that solutes from endosomes or the cytosol, such as ions can access the viral DNA. *In vivo*, the removal of the pentameric capsomers is initiated at the cell surface and continues in the endosomes.[25] Our slow unpacking experiments with the combined TIRF-AFM instrument are fully consistent with these observations by proving that the removal of only one capsomer sufficed to expose the viral dsDNA to the YOYO-1 molecules in the buffer.

Our fast unpacking experiments allow particle decapsulation and tracking of the genome release on the sub-second timescale. *In vivo* about 60 minutes pass between the uptake of the virus and DNA release into the nucleus.[27, 60-62] The disruption of the capsid at the nuclear pore complex likely happens much faster, owing to several virus uncoating and transport steps that are upstream of the nuclear pore complex, the site of capsid disruption.[17, 25, 63, 64] The main driver of capsid disassembly at the nuclear pore complex is the conventional kinesin motor[10], which has a stepping time of about 10 ms.[65] The temporal resolution of our fast unpacking experiments could be realistically increased by an order of magnitude by performing faster force curves and using higher video frame rates. The unpacking experiments showed directly the differences in condensation between the mature and immature adenovirus cores. The mature core was more accessible to YOYO-1 molecules and showed a larger spreading after fast unpacking. The spatial expansion of the mature genome occurs immediately after unpacking which indicates that it is kept under stress when packed. Indeed, AFM measurements have shown a ≈20 % increase in the stiffness of mature adenovirus over the immature particle[28], which suggests an internal pressure that is exerted by the confined genome. Interestingly, our measurements show that although the mature core expands more, it still retains a somewhat compact organization and does not completely unfold. Although this might be influenced by the affinity of the genome for the

remaining surface-bound capsid proteins, it is intriguing that also tracking of single adenoviruses in infected cells showed that many uncoated viral genomes remained in the cytosol and did not enter the nucleus[27]. The altered organization of the viral core upon maturation most likely results from the cleavage of the core proteins. Follow-up experiments with labeled core proteins in combination with experiments that probe the condensing effects of the core proteins on DNA[66] may help to reveal the molecular details of this process. More structural details about the organization of the viral DNA may also be obtained by super resolution techniques that exploit the activation of the YOYO-1 dye after binding the DNA.[67] However, this would necessitate a change of experimental procedure to immobilize the viruses. The currently used mica limits the optical performance (figure S2).

The reported expansion of the mature adenovirus genome might provide the mature core with the essential flexibility to pass through the narrow nuclear pore complex, which would contribute to infectivity. The uncoating of the adenovirus *in vivo* is more complicated than the AFM induced disassembly and involves a combination of chemical and mechanical cues that are spatially and temporally ordered. Our *in vitro* approach, with a controlled set of parameters, could be extended to further unravel the complexities of virus uncoating. Mechanical uncoating experiments could for example be performed under different chemical conditions and AFM pulling experiments[68] could be designed to mimic more closely the pulling force of the motor proteins at the nuclear pore complex or at the plasma membrane.[9, 10] The approach described here can be readily applied to study the uncoating processes of other viruses. An interesting application would be to test *in vitro* properties of artificial nanoparticles designed for drug delivery. The presented combination of single molecule fluorescence and AFM-unpacking technique, which can be performed under controlled environmental conditions, would allow monitoring drug release from engineered carriers by testing different chemical and mechanical conditions that mimic conditions in the targeted cellular environment.

## Methods

*Virus preparation*

Wildtype HAdV-C2 and the mutant HAdV-C2_TS1 were grown in A549 (human lung carcinoma) and KB (HeLa-subclone) cells, respectively, and purified as previously described [25]. Protein concentration of stock wild type virus was 1.7 µg/µl and that of TS1 0.13 µg/µl.

Wild-type (wt) particles and ts1 mutants were diluted from the stock solution to ≈2 ng/µl in Tris buffer (10 mM Tris-HCl pH 8.1, 150 mM NaCl, 1mM $MgCl_2$) plus 10% glycerol and stored at -80ºC in single-sample aliquots of 20 µL.

*Sample preparation*

A very thin (~ tens of µm) circular punched mica slice was glued with an optical adhesive to a coverslip. The refractive index of the optical adhesive (1.54, Norland products, NJ, USA) was chosen between that of mica (1.55-1.62) and the microscope coverslip (1.53) to ensure total internal reflection at the mica buffer interface.

One virus aliquot was diluted 4x in Tris buffer plus 5 mM $NiCl_2$. 40 µl of this dilution was adsorbed onto the freshly cleaved mica for 10 minutes. The microscope coverslip was placed in its holder and mounted on the xy scanning stage of the AFM that was placed on top of a custom made inverted optical microscope. YOYO-1 (Life Technologies, CA, USA) was added to 300 nM to detect the release of DNA via fluorescence microscopy.

*AFM scanning*

The AFM head, scanning stage and electronics were from Asylum Research (MFP-3D, CA, USA). The AFM was mounted on top of a custom made inverted optical microscope. The combined microscope was placed onto an active vibration isolation (Nano 30, Accurion GmbH, Göttingen, Germany) within an acoustic enclosure (AEK-2002, Herzan, CA, USA). All heat and noise generating parts (power supplies, EM-CCD, laser) were mounted outside of the enclosure and were mechanically decoupled from the AFM. Rectangular cantilevers RC800PSA (Olympus, Tokyo, Japan) with nominal spring constant of 0.39 N/m were used in amplitude modulation mode at an oscillation amplitude of less than 10 nm at ≈15 kHz. The disassembly state of the viruses was checked from 400 x 400 nm scans of the viruses in buffer. Fatigue experiments were

performed with similar settings to image acquisition. To fast unpack the viruses force curves were performed at a speed of ≈0.4 μm/s and a maximum force of ~15 nN.

*TIRF imaging*

The inverted optical microscope was custom built around a TIRF objective (100x, NA 1.49, Nikon Instruments, Japan) that was mounted on a closed piezo z-scanner (100 μm range, Physik Instrumente, Germany). Dicroic and emission filters, optimized for YOYO-1, were obtained from Semrock (NY, USA), the 488 nm laser diode from Nichia (Japan) and all optomechanical parts and lenses from Thorlabs (NJ, USA). To find the approximate position of the tip, first a bright field image was recorded. The exact position was obtained from a fluorescence image at a light angle of 0°, such that the tip apex was visible as a bright dot. For the actual capsid unpacking experiments the light angle was set at 64° to eliminate the background signal from the AFM probe.

To synchronize the AFM and fluorescence data acquisition during the unpacking experiments a routine was implemented in the AFM controller software to generate a trigger for the EM-CCD camera (Luca S-659 cooled EM-CCD, Andor technology, UK). The exposure time was 100 ms, which resulted in an acquisition frame rate of 7.5 Hz. The cooling of the CCD chip was set at -30 °C and the EM gain at 300 x. The fluorescence emission was quantified by accumulating the intensity of a 15 x 15 pixel region of interest (pixel size = 100 nm) encompassing the fluorescent spot. To obtain the intensities shown in figure 3, 10 frames were averaged after each AFM scan. Fitting of the fluorescent spots with a 2D Gaussian function was performed with Igor (Wavemetrics, USA), where $z_0$ is the noise floor, $x_0$, $y_0$ the center and $A$ the amplitude of the spot. The *width* is the reported parameter:

$$f(x,y) = z_0 + A\exp\left(-\left(\frac{(x-x_0)^2}{width}\right)+\left(\frac{(y-y_0)^2}{width}\right)\right)$$

**Supporting Information**

2 figures and 2 movies

**Acknowledgements**

P.J.P. acknowledges funding by MINECO of Spain through projects FIS2011-29493, FIS2014-59562-R and the Spanish Interdisciplinary Network on the Biophysics of Viruses (Biofivinet, FIS2011-16090-E). C.S.M. acknowledges MINECO grants BFU2013-41249-P and Biofivinet. K.B. and the single molecule fluorescence microscope were financially supported by the German Research Foundation (DFG: SFB860). I.A.T.S was funded by the Cluster of Excellence and DFG Research Center Nanoscale Microscopy and Molecular Physiology of the Brain. U.F.G. and M.S. were supported by grants from the Swiss National Science Foundation (31003A_141222/1 and 310030B_160316) and the Kanton Zurich.

**Author contributions**

A.O.E and K.B. performed experiments and analyzed data. K.B and I.A.T.S designed the combined microscope. M.S. prepared the samples and performed biochemical control experiments for the AFM-TIRF experiments. C.S.M. prepared samples and performed control experiments for initial experiments. U.F.G, P.J.P and I.A.T.S supervised the experiments and interpreted results. P.J.P. proposed the application of the AFM-TIRF for viral mechanics, and together with I.A.T.S., C.S.M. and U.F.G. designed the experiments. P.J.P., I.A.T.S. and U.F.G. composed the manuscript and all authors contributed in writing the manuscript.

## References


1. Flint, S. J.; Enquist, L. W.; Racaniello, V. R.; Skalka, A. M. *Principles of virology*. ASM Press: Washington D.C., 2004.
2. Singh, R.; Kostarelos, K. Designer adenoviruses for nanomedicine and nanodiagnostics. *Trends in Biotechnology* 2009, 27, 220-229.
3. Uchida, M.; Douglas, T. Biophysical chemistry: unravelling capsid transformations. *Nat Chem* 2013, 5, 444-5.
4. Flatt, W. F.; Greber, U. F. Misdelivery at the Nuclear Pore Complex - Stopping a virus Dead in its Tracks. *Cells* 2015, in press.
5. Mateu, M. G. Virus engineering: functionalization and stabilization. *Protein Eng Des Sel* 2011, 24, 53-63.
6. Wetz, K.; Kucinski, T. Influence of different ionic and pH environments on structural alterations of poliovirus and their possible relation to virus uncoating. *The Journal of general virology* 1991, 72 ( Pt 10), 2541-4.
7. Wilts, B. D.; Schaap, I. A.; Schmidt, C. F. Swelling and softening of the cowpea chlorotic mottle virus in response to pH shifts. *Biophys J* 2015, 108, 2541-9.
8. Banerjee, I.; Miyake, Y.; Nobs, S. P.; Schneider, C.; Horvath, P.; Kopf, M.; Matthias, P.; Helenius, A.; Yamauchi, Y. Influenza A virus uses the aggresome processing machinery for host cell entry. *Science (New York, N.Y* 2014, 346, 473-7.
9. Burckhardt, C. J.; Suomalainen, M.; Schoenenberger, P.; Boucke, K.; Hemmi, S.; Greber, U. F. Drifting motions of the adenovirus receptor CAR and immobile integrins initiate virus uncoating and membrane lytic protein exposure. *Cell host & microbe* 2011, 10, 105-17.
10. Strunze, S.; Engelke, M. F.; Wang, I. H.; Puntener, D.; Boucke, K.; Schleich, S.; Way, M.; Schoenenberger, P.; Burckhardt, C. J.; Greber, U. F. Kinesin-1-Mediated Capsid Disassembly and Disruption of the Nuclear Pore Complex Promote Virus Infection. *Cell host & microbe* 2011, 10, 210-223.
11. Suomalainen, M.; Greber, U. F. Uncoating of non-enveloped viruses. *Curr Opin Virol* 2013, 3, 27-33.
12. Canady, M. A.; Tihova, M.; Hanzlik, T. N.; Johnson, J. E.; Yeager, M. Large conformational changes in the maturation of a simple RNA virus, nudaurelia capensis omega virus (NomegaV). *Journal of molecular biology* 2000, 299, 573-84.
13. Hindiyeh, M.; Li, Q. H.; Basavappa, R.; Hogle, J. M.; Chow, M. Poliovirus mutants at histidine 195 of VP2 do not cleave VP0 into VP2 and VP4. *Journal of virology* 1999, 73, 9072-9.
14. Pang, H. B.; Hevroni, L.; Kol, N.; Eckert, D. M.; Tsvitov, M.; Kay, M. S.; Rousso, I. Virion stiffness regulates immature HIV-1 entry. *Retrovirology* 2013, 10, 4.
15. Schneemann, A.; Zhong, W.; Gallagher, T. M.; Rueckert, R. R. Maturation cleavage required for infectivity of a nodavirus. *Journal of virology* 1992, 66, 6728-34.
16. San Martin, C. Latest insights on adenovirus structure and assembly. *Viruses* 2012, 4, 847-77.
17. Nakano, M. Y.; Boucke, K.; Suomalainen, M.; Stidwill, R. P.; Greber, U. F. The first step of adenovirus type 2 disassembly occurs at the cell surface, independently of endocytosis and escape to the cytosol. *Journal of virology* 2000, 74, 7085-95.
18. Wodrich, H.; Henaff, D.; Jammart, B.; Segura-Morales, C.; Seelmeir, S.; Coux, O.; Ruzsics, Z.; Wiethoff, C. M.; Kremer, E. J. A capsid-encoded PPxY-motif facilitates adenovirus entry. *PLoS pathogens* 2010, 6, e1000808.
19. Luisoni, S.; Suomalainen, M.; Boucke, K.; Tanner, L. B.; Wenk, M. R.; Guan, X. L.; Grzybek, M.; Coskun, U.; Greber, U. F. Co-option of Membrane Wounding Enables Virus Penetration into Cells. *Cell host & microbe* 2015, 18, 75-85.

20. Gastaldelli, M.; Imelli, N.; Boucke, K.; Amstutz, B.; Meier, O.; Greber, U. F. Infectious adenovirus type 2 transport through early but not late endosomes. *Traffic (Copenhagen, Denmark)* 2008, 9, 2265-78.
21. Suomalainen, M.; Luisoni, S.; Boucke, K.; Bianchi, S.; Engel, D. A.; Greber, U. F. A direct and versatile assay measuring membrane penetration of adenovirus in single cells. *Journal of virology* 2013, 87, 12367-79.
22. Wiethoff, C. M.; Wodrich, H.; Gerace, L.; Nemerow, G. R. Adenovirus protein VI mediates membrane disruption following capsid disassembly. *Journal of virology* 2005, 79, 1992-2000.
23. Bremner, K. H.; Scherer, J.; Yi, J.; Vershinin, M.; Gross, S. P.; Vallee, R. B. Adenovirus transport via direct interaction of cytoplasmic dynein with the viral capsid hexon subunit. *Cell host & microbe* 2009, 6, 523-35.
24. Engelke, M. F.; Burckhardt, C. J.; Morf, M. K.; Greber, U. F. The dynactin complex enhances the speed of microtubule-dependent motions of adenovirus both towards and away from the nucleus. *Viruses* 2011, 3, 233-53.
25. Greber, U. F.; Willetts, M.; Webster, P.; Helenius, A. Stepwise Dismantling of Adenovirus-2 during Entry into Cells. *Cell* 1993, 75, 477-486.
26. Suomalainen, M.; Nakano, M. Y.; Keller, S.; Boucke, K.; Stidwill, R. P.; Greber, U. F. Microtubule-dependent plus- and minus end-directed motilities are competing processes for nuclear targeting of adenovirus. *The Journal of cell biology* 1999, 144, 657-72.
27. Wang, I. H.; Suomalainen, M.; Andriasyan, V.; Kilcher, S.; Mercer, J.; Neef, A.; Luedtke, N. W.; Greber, U. F. Tracking viral genomes in host cells at single-molecule resolution. *Cell host & microbe* 2013, 14, 468-80.
28. Pérez-Berná, A. J.; Ortega-Esteban, A.; Menéndez-Conejero, R.; Winkler, D. C.; Menéndez, M.; Steven, A. C.; Flint, S. J.; de Pablo, P. J.; San Martín, C. The role of capsid maturation on adenovirus priming for sequential uncoating. *J Biol Chem* 2012, 287, 31582-95.
29. Roos, W. H.; Bruinsma, R.; Wuite, G. J. L. Physical virology. *Nature Physics* 2010, 6, 733-743.
30. de Pablo, P. J.; Schaap, I. A. T.; MacKintosh, F. C.; Schmidt, C. F. Deformation and collapse of microtubules on the nanometer scale. *Physical Review Letters* 2003, 91, 98101.
31. Ivanovska, I. L.; Pablo, P. J. C.; Ibarra, B.; Sgalari, G.; MacKintosh, F. C.; Carrascosa, J. L.; Schmidt, C. F.; Wuite, G. J. L. Bacteriophage capsids: Tough nanoshells with complex elastic properties. *Proceedings of the National Academy of Sciences of the United States of America* 2004, 101, 7600-7605.
32. Liashkovich, I.; Hafezi, W.; Kuhn, J. E.; Oberleithner, H.; Kramer, A.; Shahin, V. Exceptional mechanical and structural stability of HSV-1 unveiled with fluid atomic force microscopy. *Journal of cell science* 2008, 121, 2287-92.
33. Snijder, J.; Uetrecht, C.; Rose, R. J.; Sanchez-Eugenia, R.; Marti, G. A.; Agirre, J.; Guerin, D. M.; Wuite, G. J.; Heck, A. J.; Roos, W. H. Probing the biophysical interplay between a viral genome and its capsid. *Nat Chem* 2013, 5, 502-9.
34. Hernando-Perez, M.; Pascual, E.; Aznar, M.; Ionel, A.; Caston, J. R.; Luque, A.; Carrascosa, J. L.; Reguera, D.; de Pablo, P. J. The interplay between mechanics and stability of viral cages. *Nanoscale* 2014, 6, 2702-2709.
35. Li, S.; Sieben, C.; Ludwig, K.; Hofer, C. T.; Chiantia, S.; Herrmann, A.; Eghiaian, F.; Schaap, I. A. pH-Controlled two-step uncoating of influenza virus. *Biophys J* 2014, 106, 1447-56.
36. Ortega-Esteban, A.; Pérez-Berná, A. J.; Menéndez-Conejero, R.; Flint, S. J.; San Martín, C.; de Pablo, P. J. Monitoring dynamics of human adenovirus disassembly induced by mechanical fatigue. *Scientific reports* 2013, 3, 1434.
37. Benevento, M.; Di Palma, S.; Snijder, J.; Moyer, C. L.; Reddy, V. S.; Nemerow, G. R.; Heck, A. J. Adenovirus composition, proteolysis, and disassembly studied by in-depth qualitative and quantitative proteomics. *J Biol Chem* 2014, 289, 11421-30.

38. Brown, D. T.; Westphal, M.; Burlingham, B. T.; Winterhoff, U.; Doerfler, W. Structure and composition of the adenovirus type 2 core. *Journal of virology* 1975, 16, 366-87.
39. Mirza, M. A.; Weber, J. Structure of adenovirus chromatin. *Biochim Biophys Acta* 1982, 696, 76-86.
40. Perez-Berna, A. J.; Marion, S.; Chichon, F. J.; Fernandez, J. J.; Winkler, D. C.; Carrascosa, J. L.; Steven, A. C.; Siber, A.; San Martin, C. Distribution of DNA-condensing protein complexes in the adenovirus core. *Nucleic acids research* 2015, 43, 4274-83.
41. Vayda, M. E.; Rogers, A. E.; Flint, S. J. The structure of nucleoprotein cores released from adenovirions. *Nucleic acids research* 1983, 11, 441-60.
42. Mangel, W. F.; San Martin, C. Structure, function and dynamics in adenovirus maturation. *Viruses* 2014, 6, 4536-70.
43. Weber, J. Genetic analysis of adenovirus type 2 III. Temperature sensitivity of processing viral proteins. *Journal of virology* 1976, 17, 462-71.
44. Blainey, P. C.; Graziano, V.; Pérez-Berná, A. J.; McGrath, W. J.; Flint, S. J.; San Martín, C.; Xie, X. S.; Mangel, W. F. Regulation of a Viral Proteinase by a Peptide and DNA in One-dimensional Space: IV. Viral proteinase slides along DNA to locate and process its substrates. *J Biol Chem* 2013, 288, 2092-102.
45. Pérez-Berná, A. J.; Marabini, R.; Scheres, S. H.; Menéndez-Conejero, R.; Dmitriev, I. P.; Curiel, D. T.; Mangel, W. F.; Flint, S. J.; San Martín, C. Structure and uncoating of immature adenovirus. *Journal of molecular biology* 2009, 392, 547-57.
46. Cordova, J. C.; Das, D. K.; Manning, H. W.; Lang, M. J. Combining single-molecule manipulation and single-molecule detection. *Curr Opin Struct Biol* 2014, 28, 142-8.
47. Kellermayer, M. S.; Karsai, A.; Kengyel, A.; Nagy, A.; Bianco, P.; Huber, T.; Kulcsar, A.; Niedetzky, C.; Proksch, R.; Grama, L. Spatially and temporally synchronized atomic force and total internal reflection fluorescence microscopy for imaging and manipulating cells and biomolecules. *Biophys J* 2006, 91, 2665-77.
48. Sarkar, A.; Robertson, R. B.; Fernandez, J. M. Simultaneous atomic force microscope and fluorescence measurements of protein unfolding using a calibrated evanescent wave. *Proc Natl Acad Sci U S A* 2004, 101, 12882-6.
49. Gaiduk, A.; Kuhnemuth, R.; Antonik, M.; Seidel, C. A. Optical characteristics of atomic force microscopy tips for single-molecule fluorescence applications. *Chemphyschem* 2005, 6, 976-83.
50. Rye, H. S.; Yue, S.; Wemmer, D. E.; Quesada, M. A.; Haugland, R. P.; Mathies, R. A.; Glazer, A. N. Stable fluorescent complexes of double-stranded DNA with bis-intercalating asymmetric cyanine dyes: properties and applications. *Nucleic acids research* 1992, 20, 2803-12.
51. Akerman, B.; Tuite, E. Single- and double-strand photocleavage of DNA by YO, YOYO and TOTO. *Nucleic acids research* 1996, 24, 1080-90.
52. Harrison, S. C. Structure of tomato bushy stunt virus. I. The spherically averaged electron density. *Journal of molecular biology* 1969, 42, 457-83.
53. Hendrickx, R.; Stichling, N.; Koelen, J.; Kuryk, L.; Lipiec, A.; Greber, U. F. Innate immunity to adenovirus. *Human gene therapy* 2014, 25, 265-84.
54. Andrew Knight, D.; Hickey, T. E.; Bongard, J. E.; Thach, D. C.; Yngard, R.; Chang, E. L. Differential effects of Co(III), Ni(II), and Ru(III) amine complexes on Sindbis virus. *Journal of inorganic biochemistry* 2010, 104, 592-8.
55. Grayson, P.; Evilevitch, A.; Inamdar, M. M.; Purohit, P. K.; Gelbart, W. M.; Knobler, C. M.; Phillips, R. The effect of genome length on ejection forces in bacteriophage lambda. *Virology* 2006, 348, 430-436.
56. Puntener, D.; Engelke, M. F.; Ruzsics, Z.; Strunze, S.; Wilhelm, C.; Greber, U. F. Stepwise loss of fluorescent core protein V from human adenovirus during entry into cells. *Journal of virology* 2011, 85, 481-96.

57. Grayson, P.; Han, L.; Winther, T.; Phillips, R. Real-time observations of single bacteriophage lambda DNA ejections in vitro. *Proceedings of the National Academy of Sciences of the United States of America* 2007, 104, 14652-14657.
58. Newcomb, W. W.; Cockrell, S. K.; Homa, F. L.; Brown, J. C. Polarized DNA ejection from the herpesvirus capsid. *Journal of molecular biology* 2009, 392, 885-94.
59. Ivanovska, I. L.; Miranda, R.; Carrascosa, J. L.; Wuite, G. J. L.; Schmidt, C. F. Discrete fracture patterns of virus shells reveal mechanical building blocks. *Proceedings of the National Academy of Sciences of the United States of America* 2011, 108, 12611-12616.
60. Greber, U. F.; Suomalainen, M.; Stidwill, R. P.; Boucke, K.; Ebersold, M. W.; Helenius, A. The role of the nuclear pore complex in adenovirus DNA entry. *The EMBO journal* 1997, 16, 5998-6007.
61. Lyon, M.; Chardonnet, Y.; Dales, S. Early events in the interaction of adenoviruses with HeLa cells. V. Polypeptides associated with the penetrating inoculum. *Virology* 1978, 87, 81-8.
62. Trotman, L. C.; Mosberger, N.; Fornerod, M.; Stidwill, R. P.; Greber, U. F. Import of adenovirus DNA involves the nuclear pore complex receptor CAN/Nup214 and histone H1. *Nature cell biology* 2001, 3, 1092-100.
63. Lutschg, V.; Boucke, K.; Hemmi, S.; Greber, U. F. Chemotactic antiviral cytokines promote infectious apical entry of human adenovirus into polarized epithelial cells. *Nature communications* 2011, 2, 391.
64. Wolfrum, N.; Greber, U. F. Adenovirus signalling in entry. *Cellular microbiology* 2013, 15, 53-62.
65. Svoboda, K.; Schmidt, C. F.; Schnapp, B. J.; Block, S. M. Direct observation of kinesin stepping by optical trapping interferometry. *Nature* 1993, 365, 721-7.
66. Dame, R. T.; Noom, M. C.; Wuite, G. J. Bacterial chromatin organization by H-NS protein unravelled using dual DNA manipulation. *Nature* 2006, 444, 387-90.
67. Wang, Y.; Maharana, S.; Wang, M. D.; Shivashankar, G. V. Super-resolution microscopy reveals decondensed chromatin structure at transcription sites. *Scientific reports* 2014, 4, 4477.
68. Allison, D. P.; Hinterdorfer, P.; Han, W. Biomolecular force measurements and the atomic force microscope. *Current opinion in biotechnology* 2002, 13, 47-51.

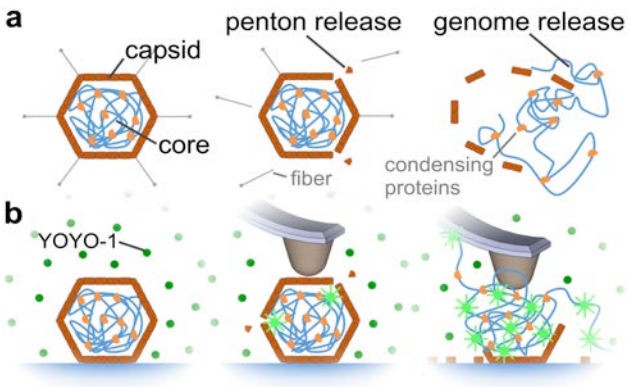


**Figure 1. Disassembly of adenovirus *in vivo* and *in vitro***

a) The hypothesized disassembly pathway of the adenovirus *in vivo*. Before disassembly the viral genome is well protected and condensed as a core within the capsid. The uptake of the virus in the target cell induces the first step of uncoating, the release of the capsid pentons. After the penton-deprived intermediate has been transported to the nuclear pore complex, the final steps of uncoating take place and the genome is released.

b) AFM-induced disassembly follows a similar sequence. First the pentons are released, followed by complete disassembly. To track the genome release, the experiments are performed in presence of YOYO-1 dye-molecules (dark green circles) that become fluorescent after binding DNA (bright green stars).

Cartoons adapted from [28, 36].

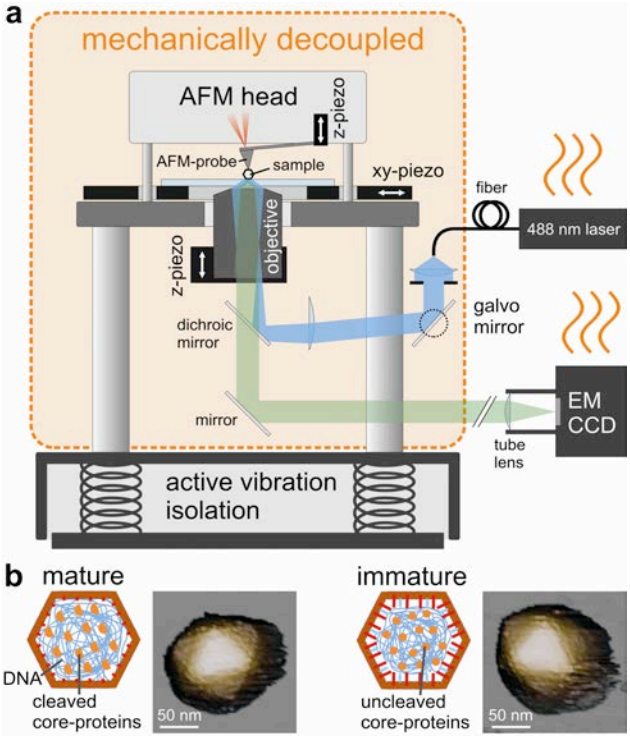


**Figure 2. Integrating TIRF with low-noise AFM.**

a) The EM-CCD camera and the laser source (both at the right) are mechanically decoupled from the AFM to prevent the transmission of noise. The AFM head rests on the custom-made inverted microscope. A microscope coverslip that holds the sample is mounted onto the AFM xy-piezo stage, such that the AFM probe has access from above. Optical access is obtained from below through a TIRF objective. Excitation of the fluorescent molecules is performed by a 488 nm laser coupled into a single-mode fiber. After collimation of the fiber output, the laser beam is coupled into the path of the optical microscope. As a first mirror we use a closed-loop adjustable galvo mirror. Because this mirror is placed in a plane that is conjugate to the focal plane, we can adjust the angle of the excitation beam. The parts of the combined microscope indicated by the orange box rest on an active vibration isolation within an acoustic enclosure.

b) The cartoons depict the condensation states of the viral cores in mature and immature particles. The core in the immature particle is more condensed because the cleavage of the core proteins did not take place. AFM scans of both types of particles showed no topographical differences of the capsids. In both cases the icosahedral symmetry is clearly visible. The diameter and height of the viruses is 95 nm, the width in the AFM scans is exaggerated due to the tip-sample dilation effect.

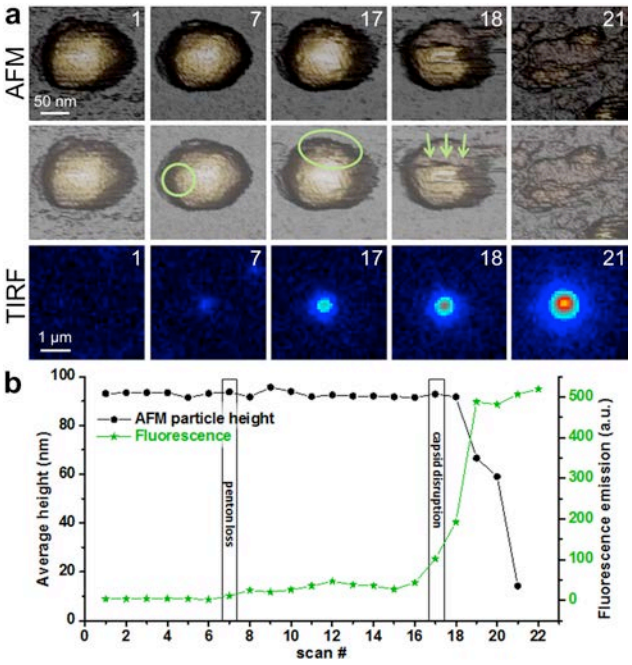


**Figure 3: Slow unpacking of adenovirus capsids.**

a) The first row shows the key AFM images of the fatigue experiment of a mature particle obtained in dynamic mode. The second row indicates the loss of the first penton in frame 7 with a circle. The ellipse in frame 17 shows the nucleation point for further disruption. The arrows indicate the direction of further disassembly in this experiment. After each AFM frame the scan was stopped, the excitation laser was switched on and 10 fluorescence images were recorded and averaged (third row). For the next AFM frame, the laser was turned off to limit bleaching of the YOYO-1 dye molecules. The time between consecutive images was 2 minutes. See also Movie S1.

b) Evolution of the average height (left axis, black) and fluorescence emission (right axis, green) corresponding to the fatigue experiment. The loss of the initial penton in frame 7 leads to a small increase in fluorescence but not to a reduction in height. The rapid decrease of height at frame 17 signals the start of the complete disassembly, accompanied by a strong increase in fluorescence.

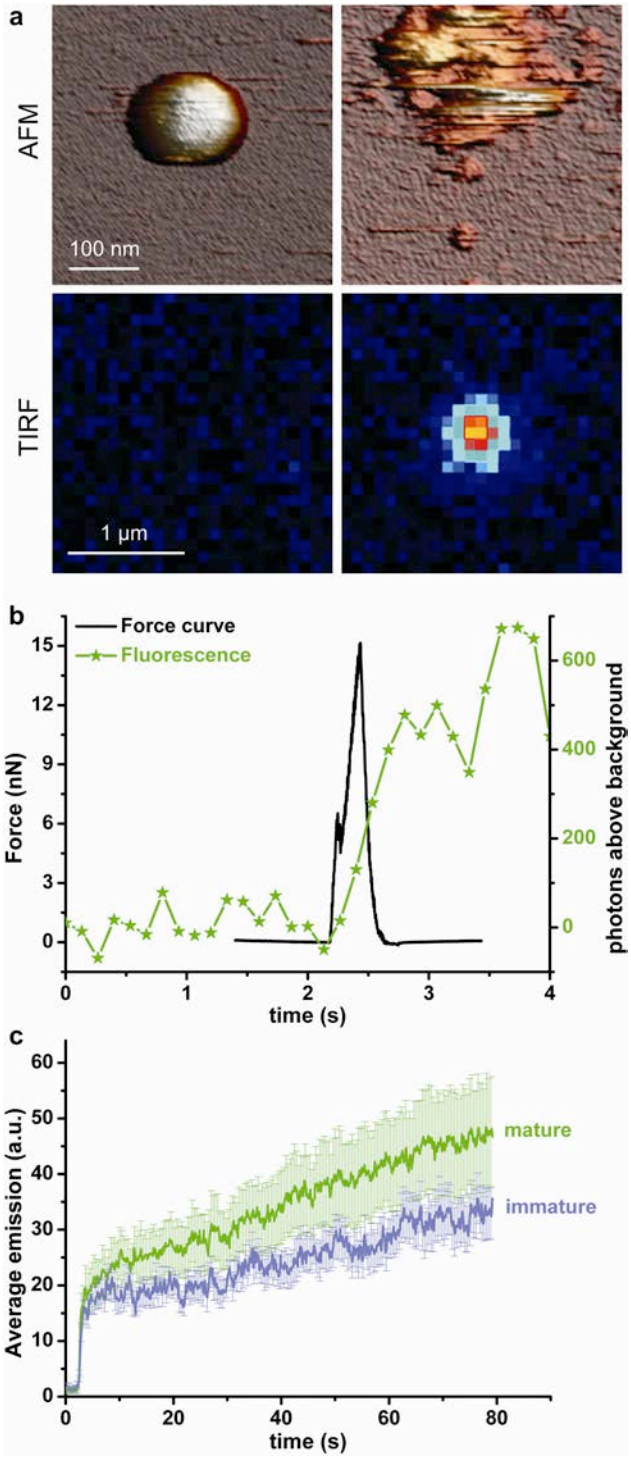


**Figure 4: Fast unpacking of adenovirus capsids.**

a) The first row shows the AFM topography of a virion before (left) and after mechanical disruption (right). The second row shows the appearance a fluorescent spot after disruption.

b) Temporal evolution of the force (left axis, black) and fluorescence (right axis, green) during the nano-indentation experiment. The intensity of fluorescence emission before the force curve

corresponds to the background noise. When the AFM tip touches the capsid (at 2.2 s) the force increases. The sudden downwards step (at 2.3 s) occurs when the AFM tip breaks the virus. Simultaneously, the fluorescence signal starts to increase. See also Movie S2.

c) The average fluorescence emission after breakage for mature (green, n=16) and immature (purple, n=17) viruses. The error bars show the standard error of the mean (SEM).

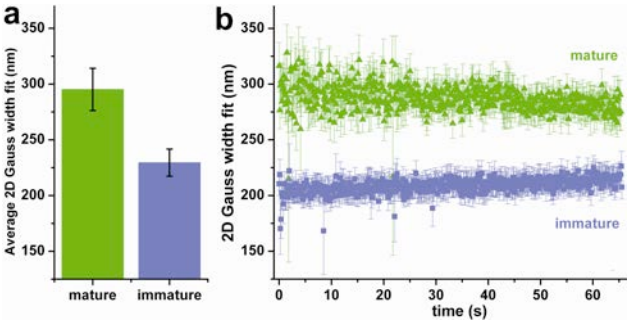


**Figure 5: The spatial spread of the mature and immature adenovirus genomes.**

a) To obtain the mean width, all frames in each fluorescence movie were averaged and the resulting image was fitted with a 2D Gauss function. The error bars show the SEM. The immature genome (blue, n=16) has a width of 229 nm. This lies in the range of what was observed in control experiments with 100 and 200 nm diameter fluorescent beads that showed widths of 208 and 253 nm, respectively (figure S2). The imaged width of the mature genome (green, n=17) is expanded by 66 nm to 295 nm.

b) To verify if the observed dilation evolves over time each individual frame was fitted with a 2D Gauss function. Each data point shows the mean of the frames from the different movies. The error bars show the SEM.